Published in final edited form as:
J Comp Neurol. 2009 June 1; 514(4): 297–309. doi:10.1002/cne.22022.

Human neural stem cell grafts in the spinal cord of SOD1 transgenic rats: differentiation and structural integration into the segmental motor circuitry

Leyan Xu[1], **David K. Ryugo**[2,3], **Tan Pongstaporn**[2], **Karl Johe**[6], and **Vassilis E. Koliatsos**[1,4,5]

[1]Department of Pathology, Division of Neuropathology, The Johns Hopkins Medical Institutions (JHMI), Baltimore, MD 21205

[2]Department of Otolaryngology, The Johns Hopkins Medical Institutions (JHMI), Baltimore, MD 21205

[3]Department of Neuroscience, The Johns Hopkins Medical Institutions (JHMI), Baltimore, MD 21205

[4]Department of Neurology, The Johns Hopkins Medical Institutions (JHMI), Baltimore, MD 21205

[5]Department of Psychiatry and Behavioral Sciences, The Johns Hopkins Medical Institutions (JHMI), Baltimore, MD 21205

[6]Neuralstem Inc., Rockville, MD

Abstract

Cell replacement strategies for degenerative and traumatic diseases of the nervous system depend on the functional integration of grafted cells into host neural circuitry, a condition necessary for the propagation of physiological signals and, perhaps, targeting of trophic support to injured neurons. We have recently shown that human neural stem cell (NSC) grafts ameliorate motor neuron disease in SOD1 transgenic rodents. Here we study structural aspects of integration of neuronally differentiated human NSCs in the motor circuitry of SOD1 G93A rats. Human NSCs were grafted into the lumbar protuberance of 8 week-old SOD1 G93A rats; results were compared to those on control Sprague-Dawley rats. Using pre-embedding immuno-EM, we found human synaptophysin (+) terminals contacting the perikarya and proximal dendrites of host α motor neurons. Synaptophysin (+) terminals had well-formed synaptic vesicles and were associated with membrane specializations primarily in the form of symmetrical synapses. To analyze the anatomy of motor circuits engaging differentiated NSCs, we injected the retrograde transneuronal tracer Bartha- pseudorabies virus (PRV) or the retrograde marker Cholera Toxin B (CTB) into the gastrocnemius muscle/sciatic nerve of SOD1 rats before disease onset and also into control rats. With this tracing, NSC-derived neurons were labeled with PRV but not CTB, a pattern suggesting that PRV entered NSC-derived neurons via transneuronal transfer from host motor neurons but not via direct transport from the host musculature. Our results indicate an advanced degree of structural integration, via functional synapses, of differentiated human NSCs into the segmental motor circuitry of SOD1– G93A rats.

Keywords

Synapse; Amyotrophic lateral sclerosis; Graft; Motor neuron

Introduction

Stem cell-based replacement therapies for neurodegenerative diseases rely, in part, on the expectation that neurons differentiated from grafted stem cells will become incorporated into circuits that support important neurological functions. This “therapeutic” integration may proceed either via the replacement of dead neurons by graft-derived, differentiated nerve cells or via the assumption of trophic and other neuroprotective functions by differentiated stem cells (Koliatsos et al., 2008). In these therapeutic scenarios, cells differentiating from the graft must establish some type of functional connectivity with host neurons.

Amyotrophic lateral sclerosis (ALS) is a neurodegenerative disease characterized by progressive neuronal death of motor neurons in the brain stem and spinal cord (Price et al., 2005). Presently available treatments are not effective and there is a particularly strong interest in experimental therapies, including cell therapies using neural stem cells (NSCs). Animal models such as transgenic rats and mice that harbor human SOD1 mutations associated with familial ALS recapitulate most pathological and clinical features of human motor neuron disease and have been extraordinarily helpful in these preclinical efforts (Wengenack et al., 2004; Aoki et al., 2005; Llado et al., 2006; Matsumoto et al., 2006). We have previously shown that human NSCs grafts in the spinal cord of SOD1 G93A rats and mice as well as in non-transgenic rodents with or without experimental lesions differentiate extensively into neurons. In SOD1 G93A rodents, these NSCs grafts protect motor neurons from degeneration, delay disease onset and prolong life span (Xu et al., 2006; Yan et al., 2006). Also, human NSCs grafts express genes encoding glial cell derived neurotrophic factor (GDNF) and brain derived neurotrophic factor (BDNF) and release these peptides in concentrations well within their trophic ranges for motor neurons (Xu et al., 2006).

In the present experiments, we explore whether human NSCs grafts form synaptic contacts with neurons of the rat motor apparatus as well as the type and extent of such contacts in the spinal cord of SOD1 G93A rats. Our results indicate that human NSC-derived neurons integrate structurally into the spinal motor circuitry of host rats, primarily via the formation of inhibitory synapses on motor and other neurons in the segmental motor apparatus.

Materials and methods

SOD1 G93A breeding

SOD1 G93A male rats from our laboratory colony were bred to Tac: N(SD) female rats from Taconic (Germantown, NY). Rats were bred in pairs of one male: one female. Offspring were weaned and genotyped at 21 days of age and positive transgenic pups were used for grafting. Colony was further propagated by breeding male pups of the same litter with the original females as described. All animal care and surgery procedures in this paper were carried out according to protocols approved by the Animal Care and Use Committee of the Johns Hopkins Medical Institutions.

Derivation and propagation of human NSCs

Human NSCs were prepared from the cervical-thoracic cord of a single 8-week human fetus as described (Yan et al., 2007). Tissues were donated by the mother in a manner compliant with NIH and FDA guidelines. Spinal cord tissues free of meninges and dorsal root ganglia were mechanically dissociated into a single cell suspension in serum-free, modified N2 medium and serially expanded in monolayer (Johe et al., 1996). Growth medium was changed every other day and, on alternate days, 10 ng/ml of bFGF was added to the culture. The first passage was performed at 16 days post-plating, a time at which the culture was comprised mostly of dividing NSCs and post-mitotic neurons. Dividing cells were harvested by brief treatment with trypsin followed by dissociation and were replated in new pre-coated

plates. Cells were harvested at ~75% confluence that occurred within 5-6 days. Process was repeated for up to 20 passages. Cells from various passages were frozen in the growth medium plus 10% DMSO in liquid nitrogen. Upon thawing, recovery rate was 80-95%.

Cells from passages 10-12 were used in this study. Five to seven days prior to surgery, one cryopreserved vial of cells was thawed, washed, and cultured again. Cells were harvested by enzymatic treatment as described above, washed in buffered saline, transferred to the surgery site on wet ice, and used within 24 hours. Viability of cells under these conditions was greater than 80%. Immediately prior to grafting, the overwhelming majority of human NSCs expressed nestin, whereas ~5% were immunoreactive for PSA-NCAM. Less than 1% of cells expressed the neuronal markers TUJ1 and MAP2 or the astroglial marker GFAP (Yan et al., 2006).

Surgical procedures

Surgical procedures were carried out under gas anesthesia (isoflurane: oxygen: nitrous oxide = 1: 33: 66) and aseptic conditions. Live or dead NSCs were grafted into the lumbar protuberance (L4 & L5) of 56 day- old SOD1 G93A rats (220-300 g; mixed gender; n=14) or Sprague-Dawley (SD) rats (220-300 g; mixed gender; n=4) mounted on a Kopf spinal stereotaxic unit under microscopic guidance. Dead cells were prepared by 3× freezing in liquid nitrogen (-70°F) and then thawing at room temperature; cell death was confirmed by a Trypan Blue uptake assay (Xu et al., 2006).

Cell suspensions were grafted with 8 injections aimed at the ventral horn on both sides of the spinal cord (1 μl with 2×10^4 NSCs per injection site, 4 injection sites per side) using pulled-beveled glass micro-pipettes connected to 10 μl Hamilton microsyringes via silastic tubing. To prevent immune rejection, all rats received FK-506 (1 mg/kg i.p. daily) till euthanized. Four SOD1 rats with live-cell grafts, 3 SOD1 rats with dead-cell grafts as well as 4 SD rats with live cell grafts were injected with Bartha-pseudorabies virus (PRV) (A gift Dr. Patrick Card, Ph.D., Department of Neuroscience, University of Pittsburgh and Dr. Lynn Enquist, Department of Molecular Biology, Princeton University) and Cholera Toxin B solution (CTB, Biological Laboratory, CA) into the right hindlimb muscles and sciatic nerve to trace motor circuitry in the spinal cord 90. The remaining animals were sacrificed after disease onset for EM analysis.

Retrograde transneuronal tracing

To assess whether grafted human NSCs can elaborate axons and establish synapses with host neurons, the retrograde transneuronal marker PRV was used to label lumbar motor neurons and nerve cells that innervate them. Fifty μl of a Bartha-PRV solution (1×10^9 plaque-forming units (pfu)/ml) were injected into the right lateral gastrocnemius muscle/ sciatic nerve of 10 SOD1 G93A rats with live or dead NSCs grafts and four 90-day old normal SD rats with live NSCs grafts. To directly compare between retrograde and transneuronal transport, after PRV injection, 5 μl of a 0.25% solution of CTB (Diluted with sterilized distilled water) were injected with a new syringe into the same gastrocnemius/ sciatic nerve site. Five days after tracer injection, rats were killed by perfusion-fixation and spinal cord segments were dissected and stored. At the time of preparation of tissues 40 days after grafting, none of the SOD1 G93A subjects displayed progressive weight loss or decrements in motor strength, i.e. signs of the symptomatic phase of SOD1 G93A-associated motor neuron disease (Xu et al., 2006).

Histology, immunocytochemistry (ICC), and microscopy

Tissues were prepared from animals perfused with fresh 4% neutral-buffered paraformaldehyde based on protocols approved by the Animal Care and Use Committee of

the Johns Hopkins Medical Institutions. Thoraco-lumbar spinal cord segments with attached roots and lumbar nerves were further fixed by immersion in the same fixative for an additional 4 hr after removing the dura. Blocks containing the entire grafted area plus 1 mm border above and below were cryoprotected and frozen for further processing. Blocks were sectioned (35 μm) at the transverse or saggital plane. In all cases, representative sections were stained with cresyl violet to study motor neuron cytology and pathology.

In most cases, dual-label immunofluorescence combined the human-specific nuclear protein antibody HNu with another cellular marker and was performed as previously described (Yan et al., 2004). Briefly, after incubation with the primary antibody overnight at 4°C, sections were treated with secondary antibodies (donkey IgG raised against the species of origin of the primary) labeled with Cy3 or Cy2 (1:200; Jackson ImmunoResearch, West Grove, PA) for 2-4 hours at room temperature. Sections were then counterstained with the fluorescent DNA dye DAPI and coverslipped with DPX. Then sections were studied with a Zeiss Axiophot microscope equipped for epifluorescence and images were captured with a Spot RT Slider digital camera (Diagnostic Instruments, Inc., Sterling Heights, MI). If the size of a region of interest was too big to be captured in one frame, a series of adjacent overlapping frames were shot under the same conditions and montaged together with the aid of Adobe PhotoShop 6.0 software (Adobe Systems, San Jose, CA). Confocal microscopic images were captured with a Zeiss LSM 510 inverted confocal microscope (Carl Zeiss, Inc.). Z-stack images from regions of interest were acquired using LSM software and then optically reconstructed at the X, Y and Z planes. To eliminate the possibility of non-specific staining with the PRV antibody, sections from animals with human NSC grafts but without PRV injections were dually stained with PRV and HNu antibodies and served as PRV ICC negative controls.

Immunoperoxidase staining for human synaptophysin was performed on sections destined for ulstrastructural analysis. Briefly, free-floating sections were processed through a series of incubations, with 0.9% phosphate-buffered saline (PBS) washes between steps, as follows: 1.5% hydrogen peroxide for 5 minutes; then incubation in 10% donkey serum for 30 minutes followed by incubation in the primary antibody (mouse anti human specific synaptophysin monoclonal antibody, 1:500) in 2.5% donkey serum at 4°C overnight; on the second day, incubation in biotinylated anti-IgG (1:200) in 2.5% donkey serum for 2 hour, then treatment with a commercially available avidin-biotin-peroxidase complex (ABC) kit for 30 minutes (Elite ABC kit PK6100, Vector, Burlingame, CA) as per manufacturer's instructions. Sections were developed with nickel-enhanced 3,3′-Diaminobenzidine (DAB) and further processed for EM.

Antibody Characterization

HNu ICC utilized a mouse monoclonal antibody (anti-human Nuclei, clone 235-1) that is directed against human interchromatin granule epitope. This monoclonal antibody reacts specifically with human cell nuclei and shows no immunoreactivity with mouse or rat cells. Antibody identifies 82 and 70 kD proteins only from human cell lysate by immunoprecipitation. (manufacturer's datasheet). Specificity of immunostaining with clone 235-1 was tested by the manufacturer on several human cell types and validated in many reports (Galli et al., 2000; McBride et al., 2004; Klein et al., 2005; Xu et al., 2006; Yan et al., 2006; Anderson and Caldwell, 2007; Yan et al., 2007).

For synaptophysin ICC, we used a mouse monoclonal antibody (anti human synaptophysin, clone EP10) directed against an epitope shared between human and hamster, but not rat, synaptophysin and raised against human synaptic immunoprecipitate. This antibody recognizes only 38 kD native human synaptophysin in peptidase digestion and deglycosylation studies. The selectivity of the antibody for human synapses has been

validated in several published studies (Guillaume et al., 2006; Xu et al., 2006; Yan et al., 2006; Cizkova et al., 2007; Yan et al., 2007).

For ChAT ICC, we used a goat polyclonal antibody raised against purified human placental ChAT. This antibody recognizes a single 68-70 kD band on Western blots from lysates of human placenta and rat basal forebrain (manufacturer's datasheet).

For PRV ICC, we used a rabbit polyclonal antibody (a gift from Dr. Patrick Card, University of Pittsburgh and Dr. Lynn Enquist, Princeton University) raised against acetone-inactivated PRV virus that recognizes all major envelope glycoproteins of PRV by immunoprecipitation and SDS-PAGE (Card et al., 1991). This antibody has been widely used in many published experiements (Card et al., 1999; Cano et al., 2001; del Rio et al., 2002; Kerman et al., 2003).

CTB ICC utilized a goat antiserum raised against the B subunit cholera toxin (choleragenoid) isolated from Vibrio cholerae type Inaba 569B. This antibody recognizes a single band of subunit B by Western blot.

Electron microscopy (EM) of human SYN-labeled synapses in ventral horn

After immunoperoxidase staining for SYN, tissue sections were treated with a solution containing 4% paraformaldehyde and 0.2% glutaraldehyde for 24 hours. Sections were then rinsed in 0.1M phosphate buffer (PB), pH 7.3, for 3 -10 minutes, immersed in 1% osmium tetroxide for 15 minutes, stained en bloc with 1% uranyl acetate for 1 hour, dehydrated in graded concentrations of ethanol, embedded in Poly/Bed 812 (Polysciences, Inc. Warrington, PA) and polymerized at 60°C for 72 hours. The ventral horn region (laminae VIII and IX) was dissected and embedded in BEEM capsules. Serial ultrathin sections were collected on Formvar-coated slotted grids and viewed with a Hitachi H-7600 transmission electron microscope equipped with a 2k × 2k bottom mount AMT-XR-100 CCD camera. Digital images were optimized for brightness/contrast and resolution (set at 600 ppi) with the aid of Adobe PhotoShop 6.0 software (Adobe Systems, San Jose, CA). To ascertain that postsynaptic structures contacted by human synaptophysin (+) terminals belonged to the host, rat motor neurons were identified by their morphology and size (>25 μm in soma diameter) and their principal dendrites were identified by tracing back to motor neuron perikarya.

The ultrastructural details of synapses originating in human NSC-derived neurons in the spinal cord of SOD1 G93A rat were studied at magnifications 15,000× or higher from sites randomly located in the ventral horn, excluding areas of NSCs engraftment. EM micrographs were randomly taken by a researcher who was blinded to the hypothesis being tested. Electron micrographs taken at the previous magnifications were used to estimate the frequencies of subtypes of membrane specializations (symmetrical versus asymmetrical) and nature of postsynaptic structure (cell body, dendritic shaft, dendritic spine). Both synapses on identified host structures (motor neurons and their principal dendrites) as well as on unidentified post-synaptic structures and synapses were counted. In the latter case, effort was made to maximize the chance of encountering host (rat) postsynaptic structures: besides avoiding areas of NSCs engraftment, we focused on post-synaptic structures that also had host synapses on them. Host-on-graft contacts are infrequent in these preparations (Xu et al., 2006; Yan et al., 2007) and, thus, the presence of rat terminals on unidentified dendrites or spines increases the possibility that these postsynaptic structures are of host origin. A total of 150 synapses were counted and percentages of symmetrical versus asymmetrical synapses to identified and unidentified post-synaptic structures were generated.

Results

Human NSC-derived neurons innervate host rat motor neurons and form structurally mature synapses with them

To distinguish between human NSCs and rat host terminals, a human-specific monoclonal antibody against synaptophysin was used. With epifluorescence microscopy, a large number of ChAT (+) host motor neurons were found to be contacted by human synaptophysin (+) terminals derived from grafted NSCs (Fig. 1A). Confocal microscopy further confirmed the apposition of terminals originating in differentiated human NSCs on host motor neurons, both their cell bodies and proximal dendrites (Fig. 1A′). The identity of these motor neurons as being of host origin is deduced from our previous findings that no graft-derived neurons differentiate fully into large motor neurons with the NSCs preparations employed in this study (Xu et al., 2006;Yan et al., 2006;Yan et al., 2007).

Based on these light microscopic findings, selected sections from grafted animals were first stained for human synaptophysin and then taken for ultrastructural analysis using standard pre-embedding protocols. Multiple synaptophysin (+) boutons with synaptic vesicles and membrane specializations were identified in the ventral horn both as *en passant* and terminal swellings. Many such synaptic structures were found to contact the cell bodies and proximal dendrites of host motor neurons (Fig. 1B-E).

Human NSC-derived neurons form circuits with themselves and with host neurons in the segmental motor system

To further characterize motor circuits engaging differentiated human NSCs, we injected PRV and CTB into the gastrocnemius muscle/distal sciatic nerve of SOD1 G93A and normal SD rats (Figs 2 and 3, respectively). PRV is a retrograde transneuronal tracer and can be transported from muscle to motor neurons and then further up to nerve cells that innervate the primarily labeled motor neurons (Kim et al., 1999;Aston-Jones and Card, 2000;Kim et al., 2002;Bareyre et al., 2004). CTB, a classical retrograde tracer, is avidly transported to nerve cells innervating muscles, including motor neurons, but not beyond these primarily labeled cells. Both markers can be used to label cell bodies in motor circuits afferent to muscle, but CTB can only label cells directly projecting to muscle.

CTB-stained preparations in SOD1 G93A rats showed a robust, but selective labeling of host motor neurons in the dorsolateral motor neuron column on the side of CTB injection (Fig. 2A). Host spinal interneurons were left unlabeled, a pattern confirming the expected classical retrograde axonal transport of CTB without further transneuronal transfer. NSC-derived neurons were also left unlabeled, a pattern suggesting that these newly differentiated neurons do not project axons into the distal sciatic nerve and that, in our NSC-grafted subjects, host motor neurons are the only source of direct projections to the periphery.

PRV-stained preparations in transgenic rats show intense labeling, primarily due to PRV immunoreactivity of NSCs grafts both ipsilateral and contralateral to the injection site (Fig. 2B). Some groups of host neurons in spinal cord other than motor neurons are also consistently labeled: such neurons are in lamina X around the central canal, where host neurons mingle with graft-derived neurons that tend to migrate to that site (Fig 2D). PRV ICC performed on sections from animals with human NSC grafts but without PRV injections (negative controls) did not yield any PRV immunoreactivity (Supplementary Fig. 4). In addition, many HNu (+) cells in grafts were not labeled with our PRV antibody (Figs 2, 3). Both patterns demonstrate that our PRV antibody does not label grafted NSCs in a non-specific fashion. In view of the innervation of host motor neurons by NSC-derived nerve cells documented in the first section of results and a lack of projection of graft-derived neurons outside the cord as shown on CTB-stained material, the intense labeling of NSC

cells with PRV particles indicates transneuronal retrograde transfer: PRV is first transported from muscle/nerve to host motor neurons and then, via the synaptic terminals of graft-derived neurons on host motor neurons, to the cell bodies of these cells in and around the graft. Further transneuronal transfer via intrinsic connections among graft-derived neurons may result in the intense labeling of the graft that is especially evident in some cases.

The role of synaptic contacts forming between NSC-derived neurons and host motor neurons as transneuronal transfer sites for PRV particles is further supported by data on normal SD rats. These animals do not show spontaneous motor neuron disease and, thus, exclude the confounding variable of motor neuron degeneration that may lead to secondary labeling of graft-derived neurons by PRV particles externalized from dying cells (Brideau et al., 2000). Patterns of retrograde labeling with CTB and RPV in normal SD rats were similar to those observed in SOD1 G93A rats (Fig. 3). As in transgenic subjects, CTB labeling was exclusive to large motor neurons in the dorsolateral column (Fig. 3A). PRV labeling was sparser in motor neurons than in graft-derived cells and the latter were labeled both ipsilateral and contralateral to the RPV injection (Fig. 3B).

Morphological appearance of synapses forming between NSC-derived and host post-synaptic structures

On the basis of light microscopic observations, many synaptic boutons belonging to graft-derived neurons contacted the cell bodies/proximal dendrites of host motor neurons. In addition to axosomatic synapses on motor neuron bodies, EM revealed that human synaptophysin (+) terminals also formed axodendritic and axospinous synapses on dendritic shafts and spines traceable to host motor neurons (Fig. 4). Some graft-derived synaptic boutons were associated with *en passant*, rather than terminal, swellings (Fig. 4D). NSC-derived neurons also formed axoaxonal synapses on host synaptic terminals on motor neuron cell bodies (Fig. 4E), a pattern suggesting that graft-derived neurons may also engage in presynaptic modulation of afferent signals to motor neurons.

The synaptic nature of these terminal or *en passant* swellings was ascertained by the presence of synaptic vesicles accumulating next to dense material on the cytoplasmic side of the terminal membrane (Schikorski and Stevens, 1999; Schikorski and Stevens, 2001), a synaptic cleft 20-30 nm wide, and the accumulation of dense cytoplasmic material on the postsynaptic membrane. Based on the thickness of postsynaptic density, synapses of human synaptophysin (+) terminals were divided into symmetrical and asymmetrical synapses; in general, symmetrical synapses are associated with inhibitory neurotransmission whereas asymmetrical synapses engage in excitatory neurotransmission (Milner et al., 1988; Peters et al., 1991; Maxwell et al., 1991; Roberts et al., 2005). More than 85% of human **s**ynaptophysin (+) boutons form symmetrical (inhibitory) synapses on motor neuron cell bodies and dendrites, a trend that is stronger in the case of axosomatic than axodendritic synapses (Fig. 4F).

Besides contacting structures identifiable as belonging to host motor neurons, a large number of graft-derived synaptic boutons were found to contact postsynaptic structures of unclear (host versus graft) origin and cellular (neuron type) identity (Fig. 5). Many such human **sy**naptophysin (+) boutons coexisted with unlabeled, for example (rat) synaptic boutons on the shafts and spines of unidentified dendrites (Fig. 5A-C). Because host-to-graft neuron synapses are rare in spinal grafts of human NSCs (Yan et al., 2004;Xu et al., 2006), we view the majority of such dually innervated shafts and spines as belonging to host dendrites. For the purpose of classification of human synaptophysin (+) synaptic profiles, we divided them into profiles that only had graft-to-host synapses and profiles that also included host-to-host (unlabeled) synapses. As in the case of synapses on identified motor neuron cell bodies and dendrites, the majority of human synaptophysin (+) terminals on ventral horn

dendrites of unknown neuronal origin formed symmetrical synapses (approximately 65% on unidentified spines and >70% on unidentified dendrite shafts) (Fig. 5D). These rates were lower than the ones on motor neuron cell bodies and dendrites.

Discussion

Results of the present study confirm and extend our previous findings showing that grafts of exogenous human NSCs in the spinal cord of normal rats as well as rodents with lesions and transgenic motor neuron disease (Xu et al., 2006; Yan et al., 2007) differentiate into populations of neurons with primarily GABAergic phenotypes that form local synapses in the ventral horn and exert neuroprotective effects for injured motor neurons (Xu et al., 2006; Yan et al., 2007). Our present findings show that neurons differentiating from grafted human NSCs form structurally mature synapses with host motor neurons and probably other cells in the segmental motor apparatus, but do not project outside the spinal cord. Synapses established between human NSC-derived neurons and host motor neurons appear to engage in efficient transneuronal transport of viral tracers from motor neurons, i.e. evidence that they are functional synapses (Irnaten et al., 2001; Carlen et al., 2002; Glatzer et al., 2003; Davis et al., 2003; Bareyre et al., 2004). The majority of these synapses, both on identified motor neurons and on unidentified dendrites in ventral horn are of the symmetrical type, i.e. synapses broadly associated with inhibitory neurotransmission (Milner et al., 1988; Peters et al., 1991; Maxwell et al., 1991; Roberts et al., 2005).

Until a few years ago, the adult spinal cord was considered an inappropriate site for stem cell grafting and differentiation because of the lack of essential inductive and neurogenic signals (Park et al., 2002). More recently, however, the spinal cord has been the target of several grafting experiments with human NSCs in healthy animals (Wu et al., 2002; Yan et al., 2004) as well as in animal models of injury and degeneration (Akiyama et al., 2001; Gao et al., 2005; Cloutier et al., 2006; Xu et al., 2006; Tarasenko et al., 2007). This persisting experimental interest is certainly related to the clinical significance of the spinal cord for illnesses as varied and severe as spinal cord injury and motor neuron disease. Initially slated to achieve the replacement of degenerating or dead motor neurons and oligodendrocytes, human NSCs have shown differentiation into motor neuron phenotypes in only a few studies (Gao et al., 2005; Zhang et al., 2006; Tarasenko et al., 2007) and efferent connections to muscle via axons extending beyond the CNS-PNS border have been especially difficult to universally demonstrate (Deshpande et al., 2006; Yan et al., 2007). On the other hand, neurons derived from NSCs in ventral horn express and secrete key trophic peptides in amounts that are within the published neuroprotective concentrations for motor neurons, including BDNF and GDNF (Llado et al., 2004; Xu et al., 2006; Suzuki et al., 2007). In some studies, stem cells have been genetically engineered with motor neuron trophic factors prior to grafting to enhance the neuroprotective effects of grafts (Blits et al., 2005; Klein et al., 2005; Suzuki et al., 2007).

The promising neuroprotective functions of NSCs grafts suggest that at least part of their therapeutic significance derives from the ability of their cell progeny to express and release motor neuron trophic signals (Xu et al., 2006). Because of the general property of trophic peptides to selectively bind to receptors expressed on the terminal but also perikaryal membranes of responsive neurons (Koliatsos et al., 1993; Davies, 2003), the ability of cells derived from human NSCs to exert trophic effects in motor neurons would depend on a proper release and transduction of trophic peptides close to target membranes via precise paracrine or transsynaptic mechanisms (Rind et al., 2005). Transsynaptic mechanisms are especially suited for neuron-to-neuron trophic effects and, in view of the primarily neuronal differentiation of NSCs in our previous work and a predominantly graft-host, as compared to host-graft, connectivity (Xu et al., 2006; Yan et al., 2006; Yan et al., 2007), they would

probably involve a transsynaptic transfer of GDNF or BDNF through terminals on host motor neurons.

Whether the goal is to replace degenerating motor neurons and directly restore information flow in the motor pathways or support injured motor neurons via the expression and release of trophic signals, integration of differentiated human NSCs into the host motor circuit via mature synapses is highly desirable. In addition to transferring key neuroprotective proteins, synapses established between graft-derived neurons and host motor neurons may also modulate motor circuits via the appropriate electric signals; inhibitory neurotransmission, in particular, may contribute to neuroprotection by "buffering" glutamatergic signals (Woo et al., 2007; Sharma, 2007). Although, in the degenerating ventral horn of G93A SOD1 rats, there is always the possibility that PRV particles can be externalized from dying motor neurons and then transported to graft-derived neurons via fluid-phase endocytosis (Brideau et al., 2000), the intense labeling of human NSC-derived neurons also in the case of SD rats is indicative of transfer via intact synapses. Further support of a transneuronal, as opposed to retrograde, transport of PRV particles to NSC-derived neurons comes from the timing of the transport and labeling experiments at 90-95 days of age of G93A transgenic rats, i.e. considerably in advance of the onset of motor neuron disease at 119-129 days. Even if few motor neurons degenerated at this early stage, it is unlikely that the amount of virus released from these dying cells would be sufficient to infect graft-derived neurons (Card et al., 1995; Card et al., 1999). In addition, most PRV virions released from necrotic neurons under these circumstances would be promptly taken up by surrounding reactive astrocytes (Card et al., 1993; Aston-Jones and Card, 2000) and thus removed from the fluid-phase pool available for terminal uptake by graft-derived neurons.

Counts of synapses of graft-derived terminals on host structures, both those associated and the ones not apparently associated with host motor neuron, showed that more than two thirds of these synapses were symmetrical, a morphology generally consistent with inhibitory neurotransmission (Milner et al., 1988; Peters et al., 1991; Maxwell et al., 1991; Roberts et al., 2005). As in other sites in the mature nervous system (Peters et al., 1991), rates of symmetrical synapses were higher in motor neuron cell bodies compared to dendrites. These results are consistent with previous findings showing that 50-60% of neurons differentiated from human NSCs grafts in the rodent spinal cord express GAD immunoreactivity in their cell bodies and terminals (Cizkova et al., 2007). The putative GABAergic transmitter identity of a majority of human NSC-derived neurons and the mature synaptic contacts of these nerve cells on host motor neurons suggest that a large percentage of cells differentiating from grafted human NSCs develop features consistent with inhibitory spinal interneurons. In fact, neurons differentiating from human NSCs may have a generic propensity to develop GABAergic phenotypes (Kabos et al., 2002; Jain et al., 2003; Kallur et al., 2006; Suon et al., 2006) and any definitive conclusions on the exact roles of human NSC-derived neurons in the segmental motor apparatus should await further studies of large and small-scale circuits in which these "new" neurons become integrated.

Both the synaptic integration of human NSC-derived neurons and their predominantly inhibitory, putatively GABAergic, neurotransmitter phenotypes help explain their therapeutic effects in motor neuron disease associated with G93A SOD1 mutations in rats and mice, including delays in disease onset and progression and prolongation of the life span of animals (Xu et al., 2006). These effects can result from transsynaptic transfer of trophic peptides or via the modulation, by these GABAergic neurons, of the excitotoxic environment in the ventral horn of G93A SOD1 rats, or both. The large number of synapses between human NSC- and host- derived neurons is also remarkable from the point of view of species origin, i.e. the fact that such a large number of "human" synapses can form on the cell body and processes of rat neurons. However, the major significance of this finding is the

remarkable malleability of human NSCs and the appropriateness of rodent subjects for further research on the preclinical potential of human NSCs to restore and protect specific neural circuits.

Supplementary Material

Refer to Web version on PubMed Central for supplementary material.

Acknowledgments

This work was supported by National Institutes of Health Grant NS45140, DC000232, EY01765, the Muscular Dystrophy Association and the Robert Packard Center for ALS Research at Johns Hopkins.

PRV and antibody are gifts from Patrick Card, Ph.D., Department of Neuroscience, University of Pittsburgh and Lynn Enquist, Ph.D., Department of Molecular Biology, Princeton University through the service of the National Center for Experimental Neuroanatomy with Neurotropic Viruses (NCRR P40 RRO118604). We wish to thank Mr Glen Hatfield for his technical help.

Reference List

Akiyama Y, Honmou O, Kato T, Uede T, Hashi K, Kocsis JD. Transplantation of clonal neural precursor cells derived from adult human brain establishes functional peripheral myelin in the rat spinal cord. Exp Neurol. 2001; 167:27–39. [PubMed: 11161590]

Anderson L, Caldwell MA. Human neural progenitor cell transplants into the subthalamic nucleus lead to functional recovery in a rat model of Parkinson's disease. Neurobiol Dis. 2007; 27:133–140. [PubMed: 17587588]

Aoki M, Kato S, Nagai M, Itoyama Y. Development of a rat model of amyotrophic lateral sclerosis expressing a human SOD1 transgene. Neuropathology. 2005; 25:365–370. [PubMed: 16382787]

Aston-Jones G, Card JP. Use of pseudorabies virus to delineate multisynaptic circuits in brain: opportunities and limitations. J Neurosci Methods. 2000; 103:51–61. [PubMed: 11074095]

Bareyre FM, Kerschensteiner M, Raineteau O, Mettenleiter TC, Weinmann O, Schwab ME. The injured spinal cord spontaneously forms a new intraspinal circuit in adult rats. Nat Neurosci. 2004; 7:269–277. [PubMed: 14966523]

Blits B, Kitay BM, Farahvar A, Caperton CV, Dietrich WD, Bunge MB. Lentiviral vector-mediated transduction of neural progenitor cells before implantation into injured spinal cord and brain to detect their migration, deliver neurotrophic factors and repair tissue. Restor Neurol Neurosci. 2005; 23:313–324. [PubMed: 16477093]

Brideau AD, Enquist LW, Tirabassi RS. The role of virion membrane protein endocytosis in the herpesvirus life cycle. J Clin Virol. 2000; 17:69–82. [PubMed: 10942087]

Cano G, Sved AF, Rinaman L, Rabin BS, Card JP. Characterization of the central nervous system innervation of the rat spleen using viral transneuronal tracing. J Comp Neurol. 2001; 439:1–18. [PubMed: 11579378]

Card JP, Dubin JR, Whealy ME, Enquist LW. Influence of infectious dose upon productive replication and transynaptic passage of pseudorabies virus in rat central nervous system. J Neurovirol. 1995; 1:349–358. [PubMed: 9222377]

Card JP, Enquist LW, Moore RY. Neuroinvasiveness of pseudorabies virus injected intracerebrally is dependent on viral concentration and terminal field density. J Comp Neurol. 1999; 407:438–452. [PubMed: 10320223]

Card JP, Rinaman L, Lynn RB, Lee BH, Meade RP, Miselis RR, Enquist LW. Pseudorabies virus infection of the rat central nervous system: ultrastructural characterization of viral replication, transport, and pathogenesis. J Neurosci. 1993; 13:2515–2539. [PubMed: 8388923]

Card JP, Whealy ME, Robbins AK, Moore RY, Enquist LW. Two alpha-herpesvirus strains are transported differentially in the rodent visual system. Neuron. 1991; 6:957–969. [PubMed: 1711350]

Carlen M, Cassidy RM, Brismar H, Smith GA, Enquist LW, Frisen J. Functional integration of adult-born neurons. Curr Biol. 2002; 12:606–608. [PubMed: 11937032]

Cizkova D, Kakinohana O, Kucharova K, Marsala S, Johe K, Hazel T, Hefferan MP, Marsala M. Functional recovery in rats with ischemic paraplegia after spinal grafting of human spinal stem cells. Neuroscience. 2007; 147:546–560. [PubMed: 17524565]

Cloutier F, Siegenthaler MM, Nistor G, Keirstead HS. Transplantation of human embryonic stem cell-derived oligodendrocyte progenitors into rat spinal cord injuries does not cause harm. Regen Med. 2006; 1:469–479. [PubMed: 17465839]

Davies AM. Regulation of neuronal survival and death by extracellular signals during development. EMBO J. 2003; 22:2537–2545. [PubMed: 12773370]

Davis SF, Williams KW, Xu W, Glatzer NR, Smith BN. Selective enhancement of synaptic inhibition by hypocretin (orexin) in rat vagal motor neurons: implications for autonomic regulation. J Neurosci. 2003; 23:3844–3854. [PubMed: 12736355]

del Rio T, Werner HC, Enquist LW. The pseudorabies virus VP22 homologue (UL49) is dispensable for virus growth in vitro and has no effect on virulence and neuronal spread in rodents. J Virol. 2002; 76:774–782. [PubMed: 11752167]

Deshpande DM, Kim YS, Martinez T, Carmen J, Dike S, Shats I, Rubin LL, Drummond J, Krishnan C, Hoke A, Maragakis N, Shefner J, Rothstein JD, Kerr DA. Recovery from paralysis in adult rats using embryonic stem cells. Ann Neurol. 2006; 60:32–44. [PubMed: 16802299]

Galli R, Borello U, Gritti A, Minasi MG, Bjornson C, Coletta M, Mora M, De Angelis MG, Fiocco R, Cossu G, Vescovi AL. Skeletal myogenic potential of human and mouse neural stem cells. Nat Neurosci. 2000; 3:986–991. [PubMed: 11017170]

Gao J, Coggeshall RE, Tarasenko YI, Wu P. Human neural stem cell-derived cholinergic neurons innervate muscle in motoneuron deficient adult rats. Neuroscience. 2005; 131:257–262. [PubMed: 15708470]

Glatzer NR, Hasney CP, Bhaskaran MD, Smith BN. Synaptic and morphologic properties in vitro of premotor rat nucleus tractus solitarius neurons labeled transneuronally from the stomach. J Comp Neurol. 2003; 464:525–539. [PubMed: 12900922]

Guillaume DJ, Johnson MA, Li XJ, Zhang SC. Human embryonic stem cell-derived neural precursors develop into neurons and integrate into the host brain. J Neurosci Res. 2006; 84:1165–1176. [PubMed: 16941479]

Irnaten M, Neff RA, Wang J, Loewy AD, Mettenleiter TC, Mendelowitz D. Activity of cardiorespiratory networks revealed by transsynaptic virus expressing GFP. J Neurophysiol. 2001; 85:435–438. [PubMed: 11152744]

Jain M, Armstrong RJ, Tyers P, Barker RA, Rosser AE. GABAergic immunoreactivity is predominant in neurons derived from expanded human neural precursor cells in vitro. Exp Neurol. 2003; 182:113–123. [PubMed: 12821381]

Johe KK, Hazel TG, Muller T, Dugich-Djordjevic MM, McKay RD. Single factors direct the differentiation of stem cells from the fetal and adult central nervous system. Genes Dev. 1996; 10:3129–3140. [PubMed: 8985182]

Kabos P, Kabosova A, Neuman T. Blocking HES1 expression initiates GABAergic differentiation and induces the expression of p21(CIP1/WAF1) in human neural stem cells. J Biol Chem. 2002; 277:8763–8766. [PubMed: 11809764]

Kallur T, Darsalia V, Lindvall O, Kokaia Z. Human fetal cortical and striatal neural stem cells generate region-specific neurons in vitro and differentiate extensively to neurons after intrastriatal transplantation in neonatal rats. J Neurosci Res. 2006; 84:1630–1644. [PubMed: 17044030]

Kerman IA, Enquist LW, Watson SJ, Yates BJ. Brainstem substrates of sympatho-motor circuitry identified using trans-synaptic tracing with pseudorabies virus recombinants. J Neurosci. 2003; 23:4657–4666. [PubMed: 12805305]

Kim ES, Kim GM, Lu X, Hsu CY, Xu XM. Neural circuitry of the adult rat central nervous system after spinal cord injury: a study using fast blue and the Bartha strain of pseudorabies virus. J Neurotrauma. 2002; 19:787–800. [PubMed: 12165138]

Kim JS, Enquist LW, Card JP. Circuit-specific coinfection of neurons in the rat central nervous system with two pseudorabies virus recombinants. J Virol. 1999; 73:9521–9531. [PubMed: 10516061]

Klein SM, Behrstock S, McHugh J, Hoffmann K, Wallace K, Suzuki M, Aebischer P, Svendsen CN. GDNF delivery using human neural progenitor cells in a rat model of ALS. Hum Gene Ther. 2005; 16:509–521. [PubMed: 15871682]

Koliatsos VE, Clatterbuck RE, Winslow JW, Cayouette MH, Price DL. Evidence that brain-derived neurotrophic factor is a trophic factor for motor neurons in vivo. Neuron. 1993; 10:359–367. [PubMed: 8080464]

Koliatsos VE, Xu L, Yan J. Human stem cell grafts as therapies for motor neuron disease. Expert Opin Biol Ther. 2008; 8:137–141. [PubMed: 18194070]

Llado J, Haenggeli C, Maragakis NJ, Snyder EY, Rothstein JD. Neural stem cells protect against glutamate-induced excitotoxicity and promote survival of injured motor neurons through the secretion of neurotrophic factors. Mol Cell Neurosci. 2004; 27:322–331. [PubMed: 15519246]

Llado J, Haenggeli C, Pardo A, Wong V, Benson L, Coccia C, Rothstein JD, Shefner JM, Maragakis NJ. Degeneration of respiratory motor neurons in the SOD1 G93A transgenic rat model of ALS. Neurobiol Dis. 2006; 21:110–118. [PubMed: 16084734]

Matsumoto A, Okada Y, Nakamichi M, Nakamura M, Toyama Y, Sobue G, Nagai M, Aoki M, Itoyama Y, Okano H. Disease progression of human SOD1 (G93A) transgenic ALS model rats. J Neurosci Res. 2006; 83:119–133. [PubMed: 16342121]

Maxwell DJ, Christie WM, Short AD, Brown AG. Direct observations of synapses between GABA-immunoreactive boutons and identified spinocervical tract neurons in the cat's spinal cord. J Comp Neurol. 1991; 307:375–392. [PubMed: 1856328]

McBride JL, Behrstock SP, Chen EY, Jakel RJ, Siegel I, Svendsen CN, Kordower JH. Human neural stem cell transplants improve motor function in a rat model of Huntington's disease. J Comp Neurol. 2004; 475:211–219. [PubMed: 15211462]

Milner TA, Morrison SF, Abate C, Reis DJ. Phenylethanolamine N-methyltransferase-containing terminals synapse directly on sympathetic preganglionic neurons in the rat. Brain Res. 1988; 448:205–222. [PubMed: 3378146]

Park KI, Ourednik J, Ourednik V, Taylor RM, Aboody KS, Auguste KI, Lachyankar MB, Redmond DE, Snyder EY. Global gene and cell replacement strategies via stem cells. Gene Ther. 2002; 9:613–624. [PubMed: 12032707]

Peters, A.; Palay, SL.; Webster, H. Synapses In The Fine Structure of the Nervous System: Neurons and Their Supporting Cells. New York: Oxford University Press; 1991. p. 138-211.

Price, DL.; Ackerley, S.; Martin, LJ.; Koliatsos, VE.; Wong, PC. Motor neuron diseases. In: Brady, ST.; Siegel, GJ.; Albers, RW.; Price, DL., editors. Basic Neurochemistry. Burlington: Elsevier; 2005. p. 731-743.

Rind HB, Butowt R, von Bartheld CS. Synaptic targeting of retrogradely transported trophic factors in motoneurons: comparison of glial cell line-derived neurotrophic factor, brain-derived neurotrophic factor, and cardiotrophin-1 with tetanus toxin. J Neurosci. 2005; 25:539–549. [PubMed: 15659589]

Roberts RC, Xu L, Roche JK, Kirkpatrick B. Ultrastructural localization of reelin in the cortex in post-mortem human brain. J Comp Neurol. 2005; 482:294–308. [PubMed: 15690491]

Schikorski T, Stevens CF. Quantitative fine-structural analysis of olfactory cortical synapses. Proc Natl Acad Sci U S A. 1999; 96:4107–4112. [PubMed: 10097171]

Schikorski T, Stevens CF. Morphological correlates of functionally defined synaptic vesicle populations. Nat Neurosci. 2001; 4:391–395. [PubMed: 11276229]

Sharma HS. Interaction between amino acid neurotransmitters and opioid receptors in hyperthermia-induced brain pathology. Prog Brain Res. 2007; 162:295–317. [PubMed: 17645925]

Suon S, Yang M, Iacovitti L. Adult human bone marrow stromal spheres express neuronal traits in vitro and in a rat model of Parkinson's disease. Brain Res. 2006; 1106:46–51. [PubMed: 16828720]

Suzuki M, McHugh J, Tork C, Shelley B, Klein SM, Aebischer P, Svendsen CN. GDNF secreting human neural progenitor cells protect dying motor neurons, but not their projection to muscle, in a rat model of familial ALS. PLoS ONE. 2007; 2:e689. [PubMed: 17668067]

Tarasenko YI, Gao J, Nie L, Johnson KM, Grady JJ, Hulsebosch CE, McAdoo DJ, Wu P. Human fetal neural stem cells grafted into contusion-injured rat spinal cords improve behavior. J Neurosci Res. 2007; 85:47–57. [PubMed: 17075895]

Wengenack TM, Holasek SS, Montano CM, Gregor D, Curran GL, Poduslo JF. Activation of programmed cell death markers in ventral horn motor neurons during early presymptomatic stages of amyotrophic lateral sclerosis in a transgenic mouse model. Brain Res. 2004; 1027:73–86. [PubMed: 15494159]

Woo RS, Li XM, Tao Y, Carpenter-Hyland E, Huang YZ, Weber J, Neiswender H, Dong XP, Wu J, Gassmann M, Lai C, Xiong WC, Gao TM, Mei L. Neuregulin-1 enhances depolarization-induced GABA release. Neuron. 2007; 54:599–610. [PubMed: 17521572]

Wu P, Ye Y, Svendsen CN. Transduction of human neural progenitor cells using recombinant adeno-associated viral vectors. Gene Ther. 2002; 9:245–255. [PubMed: 11896463]

Xu L, Yan J, Chen D, Welsh AM, Hazel T, Johe K, Hatfield G, Koliatsos VE. Human neural stem cell grafts ameliorate motor neuron disease in SOD-1 transgenic rats. Transplantation. 2006; 82:865–875. [PubMed: 17038899]

Yan J, Welsh AM, Bora SH, Snyder EY, Koliatsos VE. Differentiation and tropic/trophic effects of exogenous neural precursors in the adult spinal cord. J Comp Neurol. 2004; 480:101–114. [PubMed: 15514921]

Yan J, Xu L, Welsh AM, Chen D, Hazel T, Johe K, Koliatsos VE. Combined immunosuppressive agents or CD4 antibodies prolong survival of human neural stem cell grafts and improve disease outcomes in amyotrophic lateral sclerosis transgenic mice. Stem Cells. 2006; 24:1976–1985. [PubMed: 16644922]

Yan J, Xu L, Welsh AM, Hatfield G, Hazel T, Johe K, Koliatsos VE. Extensive neuronal differentiation of human neural stem cell grafts in adult rat spinal cord. PLoS Med. 2007; 4:e39. [PubMed: 17298165]

Zhang X, Cai J, Klueber KM, Guo Z, Lu C, Winstead WI, Qiu M, Roisen FJ. Role of transcription factors in motoneuron differentiation of adult human olfactory neuroepithelial-derived progenitors. Stem Cells. 2006; 24:434–442. [PubMed: 16141360]

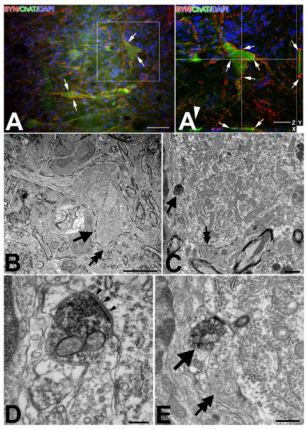

Figure 1.

Synaptic contacts between human NSC- derived neurons and host motor neurons in SOD1 G93A rats, as shown with immunofluorescence (A-A′) and immuno-electron microscopy (B-E). In all cases, human synaptophysin immunoreactivity serves as a marker for NSC-derived terminals. Postsynaptic host structures are labeled with phenotypic markers such as choline acetyltransferase (ChAT) in (A) or left unlabeled as in (B-E). The host (rat) identity of postsynaptic structure in Fig. 1 derives from the classical motor neuron morphology of post-synaptic perikarya and the fact that no human NSCs differentiate into motor neurons in these experiments.

A-A′. A large number of human synaptophysin (+) boutons (SYN, red; arrows) contact host ChAT (+) motor neurons (green). A′ is a confocal image taken from the same section as in (A) to confirm the apposition of human synaptophysin (+) boutons to the cell body and dendrites of the large motor neuron on the right of (A). Arrows in (A′) depict boutons that are further validated with x and y resectioning.

B-D. These electron photomicrographs depict, in successive enlargements, a host motor neuron (delineated with a black dashed line in [B]) contacted by a human synaptophysin immunoreactive terminal (arrow in all panels); the latter stands in comparison to an adjacent, unlabeled, host terminal (double arrow head in panels [B-C]). Panel D shows the ultrastructure of the human NSC-derived terminal replete with round synaptic boutons, mitochondria and terminal membrane specializations (arrowheads).

E. This photograph is taken from a section immediately adjacent to the one in (B-D) and showcases the same human NSC-derived synapse as panels B-D (arrow) and, in greater detail, the adjacent host-derived (unlabeled) terminal (double arrow head). Magenta-green color copy of Figure 1 is also available as Supplementary Figure 1.

Size bars: A, 50μm; A′, 20 μm; B, 10 μm; C, 1 μm; D, 0.1 μm; E, 0.5 μm

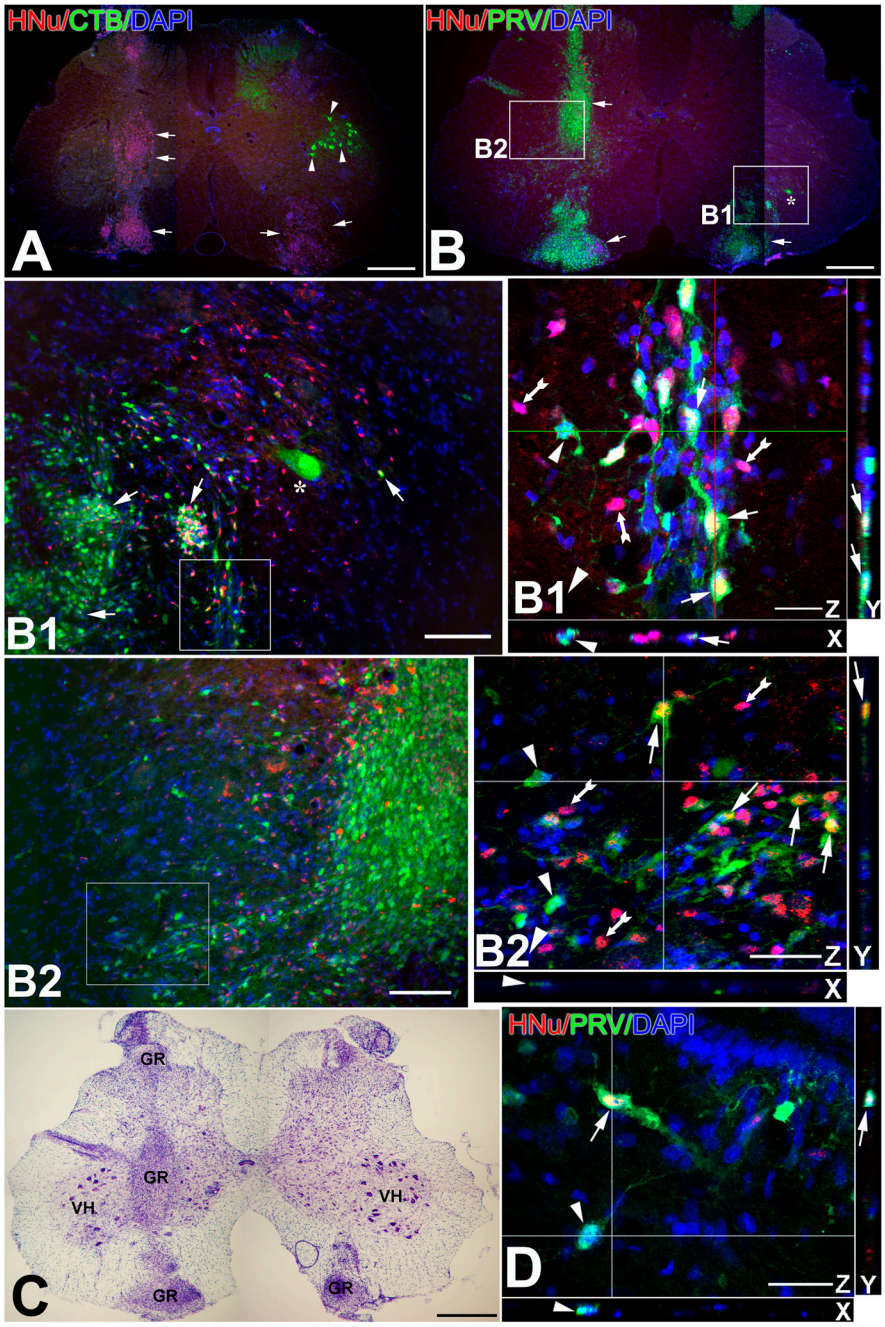

Figure 2.

Circuits engaging differentiated NSCs in SOD1 G93A rat spinal cord, as demonstrated with CBT and PRV tracing from injections into the gastrocnemius/sciatic nerve. Panels with letters-numbers represent sequential magnifications of framed areas in (B).

A-B. These two panels are taken from adjacent sections treated with CTB (A) and PRV (B) ICC and are juxtaposed to demonstrate differential patterns of labeling. In (A), note the selective CTB labeling of large motor neurons in the dorsolateral column (arrowheads) ipsilateral to the right-hand injection side and absence of any labeling in the graft (arrows pointing to HNu [red]-labeled structures). In contrast, there is sparse PRV labeling of motor

neurons (asterisk) on the side of tracer injection and an especially intense labeling of graft cells (arrows) on both sides in (B).

B1-B2′. These panels represent serial magnifications of framed areas in B and B1-2, such that (B1′) is a magnification of the framed area in (B1) and so is (B2′) with respect to (B2). Panel B1 showcases a PRV-labeled host motor neuron (asterisk) and isolated as well as clustered NSCs labeled with PRV (arrows). Panel B1′ is a confocal image showing multiple NSC-derived, PRV-labeled neurons (arrows; dually fluorescent for HNu-red and PRV-green) and many PRV (-) human NSCs (tailed arrows). Panel B2′ is a confocal image from a region where PRV-immunoreactive host neurons (arrowheads), non PRV-labeled human NSCs (tailed arrows) mingled with PRV- and HNu-labeled graft-derived neurons (arrows).

C. This cresyl-violet stained section is adjacent to sections depicted in (A-B) and serves as a guide for spinal cord anatomy including graft sites (GR) and ventral horn (VH). Note that motor neuron degeneration is not evident at this time point in the natural course of G93A motor neuron disease.

D. NSC-derived neurons (here dually labeled with HNu-red and PRV-green) in lamina X ventral to the central canal were consistently present in PRV-stained material and may have played a role for transneuronal transfer or PRV from side to side. A PRV (+) host neuron is indicated with an arrowhead, whereas a PRV (+) graft-derived neurons (also positive for HNu) is shown with an arrow.

Magenta-green color copy of Figure 2 is also available as Supplementary Figure 2.

Size bars: A, 200 μm; B, 200 μm; B1, 50 μm; B′, 10 μm; B2, 50 μm; B2′, 10 μm; C, 200 μm; D, 10 μm

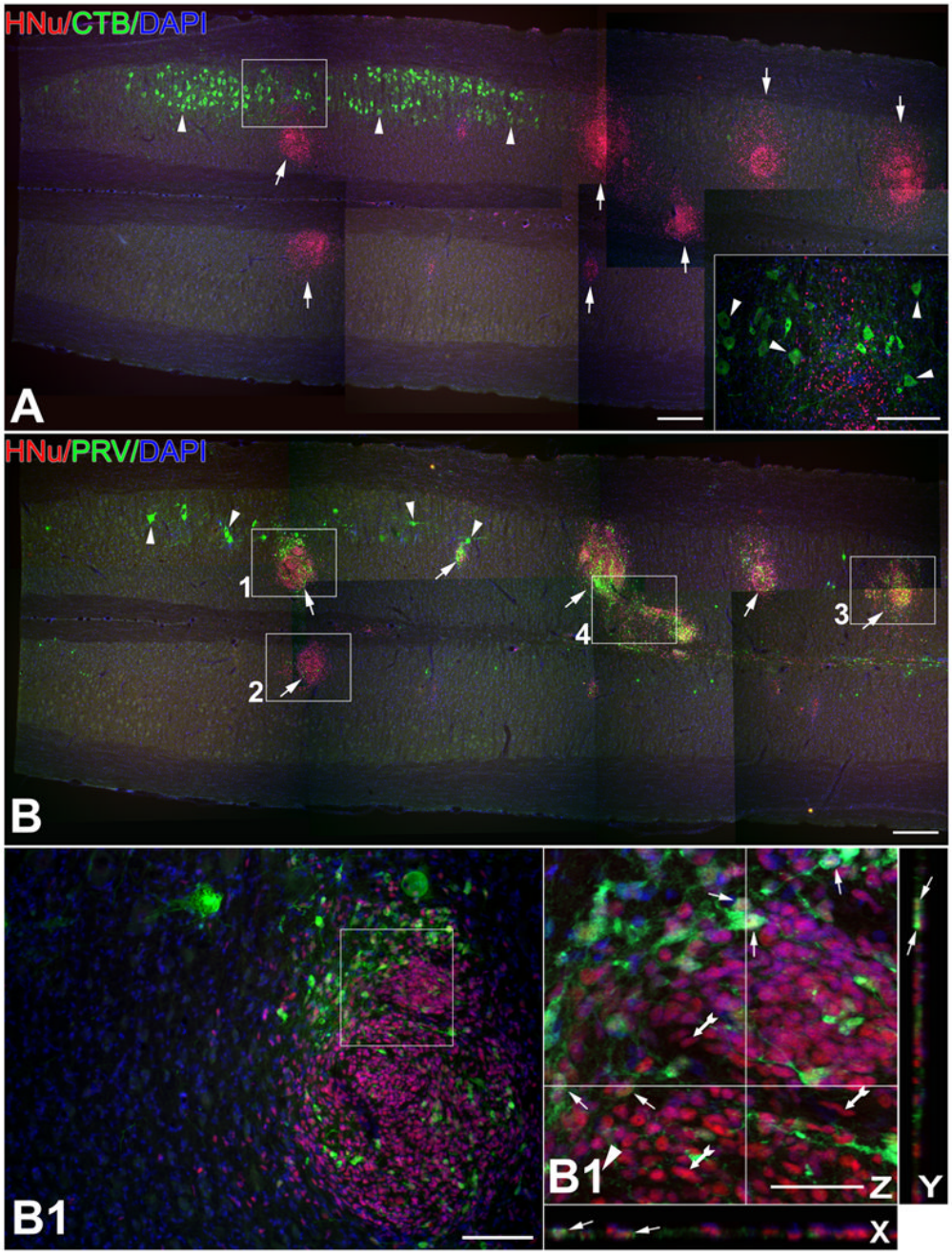

Figure 3.

Circuits engaging differentiated NSCs in the normal spinal cord of normal SD rats as demonstrated with CBT (A) and PRV (B) tracing from injections into the gastrocnemius/sciatic nerve. Panels with letters-numbers represent sequential magnifications of framed areas in (B).

A-B. These two panels are taken from adjacent longitudinal sections processed with ICC for CTB (A) and PRV (B) visualization and juxtaposed here to reveal differential patterns of labeling. (A) features the selective CTB labeling of α-motor neurons in the dorsolateral column (arrowheads) ipsilateral to the side of tracer injection and the absence of any labeling in the graft (shown here with arrows as HNu [red]-labeled structures). PRV

preparations (B), in contrast, show sparse labeling of motor neurons (arrowheads) on the injection side and intense labeling of cells in grafts (arrows). Inset represents magnification of framed area in main panel and shows a region where CTB-labeled host motor neurons (arrowheads) mingle with unlabeled, HNu (+), graft-derived cells.

B1-B4′. The four main panels (B1-B4) are magnifications of framed areas in (B) and panels further designated with a prime sign are confocal magnifications of main panels to showcase PRV-labeled, graft-derived (HNu [+]) neurons within grafts. (B2) is from the side contralateral to PRV injection. (B4) depicts a bridge between two HNu (+) inoculation sites with fusiform cells that may migrate from one site to another. Double-labeled (graft-derived) profiles are indicated with arrows and PRV (-) human NSCs are indicated with tailed arrows in all panels.

Magenta-green color copy of Figure 3 is also available as Supplementary Figure 3.

Size bars: A, 200 μm; B, 200 μm; B1, 50 μm; B1′, 10 μm; B2, 50 μm; B2′, 10 μm; B3, 50 μm; B3′, 10 μm; B4, 50 μm; B4′, 10 μm

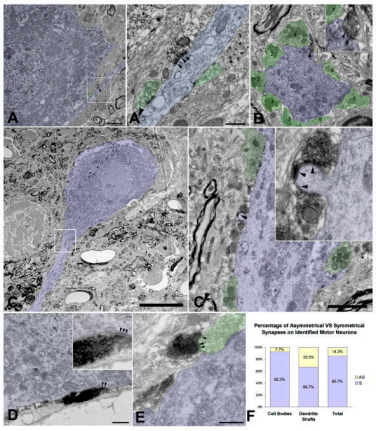

Figure 4.

Representative synaptic profiles of graft-derived, human synaptophysin (+) boutons contacting dendritic shafts and spines of identified host motor neurons. Panels labeled with a primed capital letter represent magnifications of framed areas in panels labeled with capital letter alone. Green and blue colors denote host pre- and post-synaptic structures, respectively.

A-A′. This EM photograph shows a human synaptophysin (+) terminal swelling (arrowheads) forming an axodendritic symmetrical synapse with the dendritic shaft of a host motor neuron; host synaptic terminals are also shown on the same dendrite.

B. A graft-derived, human synaptophysin (+) terminal squeezes in to form an axodendritic synapse (arrowheads) on a dendritic shaft traceable to a host motor neuron, along with 8 host-derived synapses (green). Inset represents a higher magnification of the human synaptophysin (+) terminal in main panel.

C-C′. A graft-derived terminal forms a symmetrical axospinous synapse (arrowhead) on the proximal dendrite of a host motor neuron. Inset in C′ represents a higher magnification of the labeled synapse in main panel. Spines traceable to host motor neurons are rare in our preparations.

D. This panel shows a graft-derived en passant swelling forming an asymmetrical synapse (arrowhead) with a host motor neuron cell body; inset shows detail of the synapse in higher magnification.

E. A graft-derived, human synaptophysin (+) terminal forms an axoaxonal synapse (arrowheads) on a host terminal that, in turn, synapses on to a host motor neuron.

F. A bar diagram showing percentage rates of asymmetrical (AS) versus symmetrical (S) graft derived, human synaptophysin (+) synapses on identified motor neuron postsynaptic (cell bodies and dendritic shaft; spines traceable to motor neurons are very rare).

Size bars: A, 2 μm; A1′, 0.5 μm; B, 1 μm; C, 20 μm; C′, 2 μm; D, 0.5 μm; E, 0.5 μm

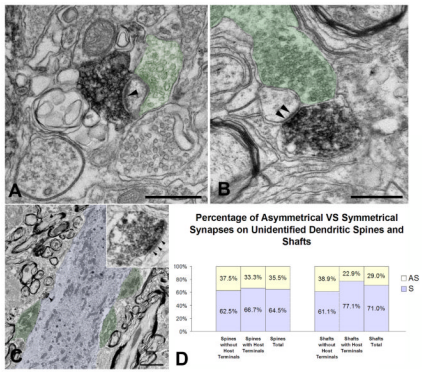

Figure 5.

Representative synaptic profiles of graft-derived terminals contacting dendritic shafts and spines in the host ventral horn that could not be traced to specific neuron types, such as motor neurons. Some of these postsynaptic structures also receive innervation by human synaptophysin (-) (host) terminals. All profiles accounted for here are far from the graft inoculation site. As in Fig. 4, green and blue colors denote host pre- and post-synaptic structures, respectively.

A-B. These two panels show graft-derived terminals forming asymmetrical (A) and symmetrical (B) axospinous synapses (arrowheads) on unidentified dendritic spines that also receive synaptic contacts from host neurons.

C. A graft-derived, human synaptophysin (+) terminal forms an asymmetrical synapse (arrowhead) with unidentified dendritic shaft. Host terminals are also shown on the same portion of the host dendrite. Inset shows further detail of the graft-to-host synapse in the main panel.

D. This bar diagram shows the percentage rates of asymmetrical (AS) versus symmetrical (S) graft derived, human synaptophysin (+) synapses on unidentified dendritic shafts and spines, further subdivided per the co-occurrence or not of host synapses in the vicinity.

Size bars: A, 0.5 μm; B, 0.5 μm; C, 2 μm

Table 1

Primary Antibodies Used

Antigen	Immunogen	Manufacturer, species, type, catalog number	Dilution used
Interchromatin granule in human cell nucleus (HNu)	Nuclear homogenate from human blood lymphcytes	Chemicon (Temecula, CA), Mouse, monoclonal, #MAB1281	1:800
Human synaptophysin	Crude human synaptic immunoprecipitate	Chemicon (Temecula, CA), Mouse, monoclonal, #MAB332	1:500
Choline acetyltransferase (ChAT)	Purified human placental ChAT	Chemicon (Temecula, CA), goat, polyclonal, #AB144P	1:100
Bartha-pseudorabies virus (PRV)	Acetone-inactivated PRV virus	Gift from Dr. Patrick Card, University of Pittsburgh and Dr. Lynn Enquist, Princeton University, rabbit, polyclonal	1:4,000
Cholera toxin B Subunit (CTB)	B subunit (choleragenoid)	List Biological Laboratory (Campbell, CA), goat, antiserum, #7032A5	1:1,000